Available online at www.sciencedirect.com

ScienceDirect

Advances in Space Research 74 (2024) 3201–3215

ADVANCES IN SPACE RESEARCH (a COSPAR publication)

www.elsevier.com/locate/asr

Shape memory polymer composite hinges for solar sails

Leandro Iorio [a,*], Fabrizio Quadrini [a], Loredana Santo [a], Christian Circi [b], Enrico Cavallini [c], Rocco Carmine Pellegrini [c]

[a] Department of Industrial Engineering, University of Rome "Tor Vergata", Via del Politecnico 1, 00133 Rome, Italy
[b] Department of Astronautical Electrical and Energy Engineering, Sapienza University of Rome, Via Salaria 851, 00138 Rome, Italy
[c] Italian Space Agency, Via del Politecnico s.n.c., 00133 Rome, Italy

Received 5 January 2024; received in revised form 29 June 2024; accepted 2 July 2024
Available online 6 July 2024

Abstract

Smart hinges for self-deployable solar sails have been prototyped by using shape memory polymer composites (SMPCs). During hinge lamination, a shape memory (SM) epoxy resin is deposited between carbon fiber reinforced (CFR) plies, and consolidation is obtained by an out-of-autoclave (OOA) process. The smart hinges have been assembled with CFR booms to prototype a small self-deployable square sail. Polymeric supports, made by fused deposition modelling (FDM), have been added for correct assembly and to drive the recovery of the SMPC hinges. Flexible heaters have been used as heating elements for SMPC hinge activation. The sail consisted of a polyimide membrane which was connected with the composite booms by flexible joints. The solar sail prototype size has been limited to 260×260 mm^2 for on-Earth testing, with 4 hinges at the middle length of the composite booms. Recovery tests have shown the ability of the smart hinges to overcome the sail weight and additional friction forces, and the small sail has been successfully deployed in laboratory. Full recovery has been achieved in less than 3 min under different configurations.
© 2024 COSPAR. Published by Elsevier B.V. This is an open access article under the CC BY-NC-ND license (http://creativecommons.org/licenses/by-nc-nd/4.0/).

Keywords: Shape Memory Polymer Composite; Solar Sail; Smart Materials; Self Deploying Structures; Non-explosive actuators

1. Introduction

The investigation of new propulsion systems suitable for long term space missions is a fundamental challenge to reduce resource consumption and aging phenomena. Propulsion systems are mainly based on propellants, both liquid or solid, but a different and very promising solution is offered by photonic (or solar) sails. In this case, the interaction with the solar radiation pressure (SRP) supplies the required energy for any mission need of space structures, as the thrust and the attitude control above all. In 2010 the Japanese Space Agency (JAXA) demonstrated the feasibility of solar sail technology thanks to the space probe IKAROS, driven-up to Venus after sail deployment (Tsuda et al., 2013). Thanks to the experience of IKAROS some technical issues have been fixed, such as the use of a square-based ultrathin and huge membrane, 7.5 μm thick and 14 m side (20 m diagonal) and the use of centrifugal forces to guarantee its deployment and flatness.

After the achievements obtained with the IKAROS experiment, space agencies all over the world have proposed other solar sail prototypes, whose testing is mainly carried out on Earth. This is the case of NASA (USA) which produced two square solar sails with the same size of IKAROS and performed tests under vacuum with optimal results (Johnson et al., 2011). Moreover, a new solar sail architecture based on a central body structure, from which 4 deployable booms start, one for each semi-diagonal, has been introduced. Because of the lack of funding, NASA directed its research on 2 subscale solar sails, NanoSail D and NanoSail D2 (Fu et al., 2016), where only

* Corresponding author.
E-mail address: leandro.iorio@uniroma2.it (L. Iorio).

https://doi.org/10.1016/j.asr.2024.07.010
0273-1177/© 2024 COSPAR. Published by Elsevier B.V.
This is an open access article under the CC BY-NC-ND license (http://creativecommons.org/licenses/by-nc-nd/4.0/).

the latter completely deployed on orbit. Further enhancements in the solar sail technology have been achieved with the introduction of the bi-stable booms, by the Surrey Space Center (UK). These booms have two stable configurations, one coiled and one extended, and adjacent booms tensioned the strips in which sail membrane is divided (Fernandez et al., 2011). The German Aerospace Center (DLR) began an experimental campaign to establish technology developments for propellant-less and high-efficient class of spacecraft for space exploration. This investigation led to the establishment of the Gossamer program where light-weight coilable booms manufactured in carbon-fiber-reinforced-polymer (CFRP) and arranged in a cross-like layout were adopted (Spietz et al., 2021). Gossamer program was divided in 3 projects: Gossamer-1, Gossamer-2 and Gossamer-3. Gossamer-1 dealt with the development of a low-cost demonstrator for membrane deployment and the adopted sail membrane was similar to that of IKAROS (Seefeldt et al., 2017a). Gossamer-2 dealt with the validation of all the related technologies on a 20×20 m^2 sail in Earth orbit and Gossamer-3 dealt with a fully functional 50×50 m^2 solar sail to validate the design approach and prove the reliability to conduct space weather mission (Grundmann et al., 2019). Several non-technical aspects limited the achievements of Gossamer-1 project which consequently influenced the successive projects and separable deployment units have been used in the end (Spietz et al., 2021).

The right operation of solar sails depends on ensuring very large and very light structures after deployment. On Earth testing of these light structures is difficult because of the gravity, conversely, small-size structures are preferred for in Space experimentation. In this case solar sails can be used as drag sail rather than propulsion systems. In fact, the drag effect of the small, deployed sail may reduce the presence of small satellites in orbit at their end-of life, and SiaSail-I, based on a 6U cubesat is a clear example of this application (Liu J. et al., 2022). The well consolidated strategy of bi-stable composite booms has been used and after a 10-year research program, the LightSail-2 mission put in orbit a large sail, 32 m^2 of surface area after full deployment (Spencer et al., 2021). Four independent triangular aluminized Mylar® sheets, 4.6 μm thick constituted the membrane whereas 4 triangular retractable and collapsible booms, made of a non-magnetic and non-corrosive alloy guaranteed the sail segments deployment. A further evolution has been obtained by the InflateSail mission, where a 3U cubesat was equipped with a 1 m long inflatable mast and a 10 m^2 deployable drag sail (Underwood et al., 2019). In this case the sail membrane was divided in 4 quadrants made of a 12 μm thick polyethylene naphthalate (PEN) film left un-metallized to limit perturbation induced by the interaction with SRP. Finally, the sail structure consisted of 4 bi-stable CFRP booms coiled just above the wrapped sail membrane.

In solar sail design, deployable strategies (Zhang et al., 2021) and manufacturing constraints strictly depend on the selection of the deployment architecture. The rise of wrinkles is the direct consequence of folding large ultra-thin metallized membrane, and propulsion efficiency can be severely reduced. In fact, wrinkles are responsible for the lack of membrane flatness upon unfolding. For designing, finite element modelling (FEM) helps in predicting the rise of wrinkles for small (Zou et al., 2022) and large sails (Santo et al., 2019). Basically, the goal is minimizing the payload volume after launch, and avoiding boom failure and sail tearing after on-orbit deployment. Packing strategies can be derived by the origami-based concept (Dang et al., 2022). The development of self-folding membranes by using space-qualified materials which deploy upon solar irradiation (Wu et al., 2018) is instead a recent trend. Anyway, finding the optimal configuration is still a difficult task and manufacturing issues are not fully considered. Moreover, different other loads, not all predictable, may arise during sail deployment (Seefeldt, 2017b) and may influence the membrane deformation. One of the first solution for sail deployment is related to inflatable booms (Genta and Brusa, 1999) which has been later successfully applied for torus-shaped solar sail consisting of a toroidal rim with an attached circular flat membrane coated by heat sensitive materials (Kezerashvili et al., 2021a). Further studies established the mathematical laws to extend the deployment and stretching of circular sail membrane attached to a toroidal shell also for large size solar sails (Kezerashvili et al., 2023). Interesting solutions in deploying solar sails are offered by smart materials which replace electromechanical actuators. Shape Memory Alloy wires made by NiTinol can be integrated in the sail membrane so providing unfolding under irradiation (Bovesecchi et al, 2019) and planarity analysis after deployment can be optimally performed through 3D Laser Scanner (Boschetto et al., 2019). Currently, carbon fiber reinforced polymeric (CFRP) booms are a valid solution because of the low weight and well consolidated manufacturing processes (Sickinger et al., 2006). On the other side, the bi-stable configurations are the most used and allow direct joining of the body sail under different geometrical constraints (Fernandez et al., 2011; Seefeldt et al., 2021). Furthermore, stress and strains arising during wrapping and deploying when using CFRP booms can be predicted again by finite element modelling (Yang et al., 2019a; Hibbert and Jordaan, 2021). Results, also show that bending and torsional stiffness of CFRP booms could be enhanced by using new configurations as the 4-cell lenticular honeycomb booms (Yang et al., 2022) or the N-shape composite ultra-thin booms (Yang et al., 2019b).

To date, IKAROS represents the state of the art in the solar sail technology despite the several developed prototypes and, the introduction of the bi-stable deploying booms opened the way towards new architectures. A very promising solution for deployable CFRP booms has been reached with a recent innovation in the field of smart CFRP materials, thanks to the adoption of shape memory polymer composites. The structural properties of CFR laminates and the functionalities of shape memory

polymers (SMPs) are combined in this new class of materials. SMPCs, as SMPs, are able to fix a stable but temporary deformed shape upon the application of a thermo-mechanical cycle and restore the initial equilibrium shape by an external stimulus, typically heating, in absence of external constraints. In SMPCs, the polymeric matrix is responsible of the SM properties whereas the reinforcements guarantee the mechanical performances. Different aerospace applications have been already proposed such as solar arrays, reflector antennas, deployable hinges, deployable panels and booms (Liu Y.J. et al., 2014) as well as a cubic deployable support (Li et al., 2016).

A recent achievement has been obtained in manufacturing CFR-SMPCs. In detail, a thin SMP layer (about 100 μm thick), is deposited between commercial CFR prepregs during lamination (Tedde et al., 2018; Quadrini et al., 2019). Moreover, co-curing of the two different resin systems is performed by compression molding. An optimal adhesion and the soundness of the manufactured smart structures have been demonstrated (Bellisario et al., 2022). The SMP resin used in these CFR-SMPCs has been already tested under microgravity in the forms of foams (Santo et al., 2012; Santo et al., 2015) and interlayer of a CFR laminate (Santo et al., 2015). A very interesting autonomous CFR-SMPC device has been obtained and is suitable to be used as actuator. In this device, a flexible heater has been embedded during composite lamination (Quadrini et al., 2021). Furthermore, these CFR-SMPCs structures can undergo to several thermo-mechanical cycles without the evidence of failures if deformation remains in the elastic range (Quadrini et al., 2022). SMPCs represent a valid alternative as deploying booms for solar sail, and preliminary results have been already discussed (Santo et al., 2019). In the current study, SMPCs have been used as active elements (actuators) connecting passive CFR elements (booms). The assembly made of SMPC actuators and CFR booms has been used as the frame of a small solar sail prototype 260 × 260 mm^2. Flexible heaters powered through a well-defined current intensity have been used to activate the SMPCs transition. In fact, the use of superconductive current-carrying wire for deployment and stretching thin membrane has been deeply investigated (Kezerashvili and Kezerashvili, 2021b). In this way, the combination between classical electrodynamics and the theory of elasticity allowed to evaluate the magnetic field induced by the superconductive current-carrying wire and the elastic properties of large sail membrane (Kezerashvili and Kezerashvili, 2022). The required stress and strain for correct deployment and mechanical stability of the sail in the deployed static configuration can be numerically derived (Kezerashvili and Kezerashvili, 2024). Supporting elements produced by fused deposition modelling drive the SMPC hinges in their final flat configuration upon recovery. Joining between the sail membrane and the external perimeter frame has been also studied to minimize the rise of wrinkles. This deploying architecture is a possible solution to be used for missions such as Helianthus, where the solar sail would be necessary to maintain an equilibrium point in the Sun-Earth gravitational field (Bassetto et al., 2022).

2. Materials and methods

The research activities have been carried out to manufacture a small sail structure, to be tested on Earth. In terms of materials and sizes, the final prototype is more similar to a drag sail for LEO. In fact, the membrane is made of a 50 μm polyimide film, much thicker than typical thin membranes of solar sails, and not aluminized. The booms are made of four CFR passive elements linked through-active SMPC hinge/Polymeric support assemblies. The whole assembly is placed on the external perimeter of the square membrane and this architecture is referred as "small deployable sail" (Fig. 1). The passive elements have been obtained by lamination of CFR prepregs and compression molding. For the SMPC hinges, SMP interlayers (nominally 150 μm thick) have been deposited between CFR plies during lamination and curing was performed through an Out of Autoclave (OOA) process (Bellisario et al., 2023). Lastly, supports have been produced by Fused Deposition Modelling. The proposed prototype architecture is suitable to investigate the main technical issues that would arise when scaling to large size solar sail. In particular, SMPC laminates should be placed only in the folding zones and properly designed joining solution has to be used to link active and passive elements.

Flexible heaters have been placed onto the smart structures and a two-step deployment strategy has been designed and implemented to avoid interferences of the membrane as well as tearing.

2.1. Raw materials and suppliers

Commercially available materials were used to produce the SMPC hinges. The CFR prepreg was M49/42 %/200-

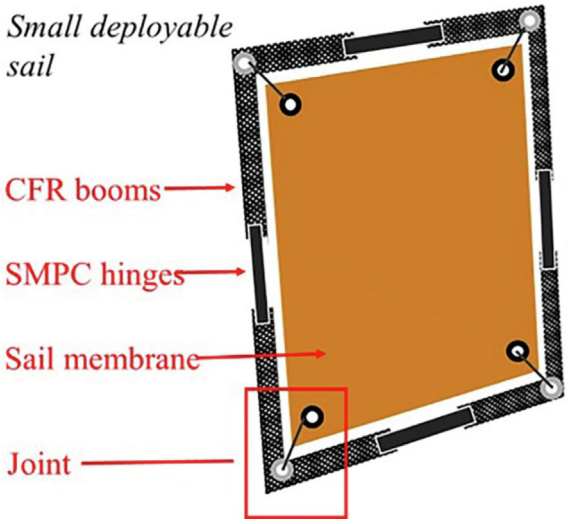

Fig. 1. Architecture of the small deployable solar sail.

PW CCF-3 k by Hexcel, commonly used for high performance structures in aeronautics. This is a 0/90 carbon fiber (CF) fabric reinforced prepreg with thermosetting epoxy matrix. This cured epoxy resin has not remarkable SM properties; therefore, a SMP interlayer was added during lamination, between CFR plies. The interlayer is in the form of an un-cured epoxy powder, commercially available and namely Scotchkote 206 N by 3 M. During lamination, the un-cured epoxy powder was deposited between adjacent CFR prepreg stripes to form a SMP interlayer with nominal thickness of 150 μm. Previous works had already discussed the good SM performances of this SMP resin in the form of foam (Santo et al., 2012; Santo et al., 2015; Quadrini et al., 2021) and in the form of CFR laminate interlayer (Tedde et al., 2018; Quadrini et al., 2019; Bellisario et al., 2022; Quadrini et al., 2022).

The sail membrane was made with a 50 μm thick polyimide film (Kapton HN) by Dupont®. This material can withstand temperatures up to 400 °C without melting or degrading and is already used for many Space applications.

The flexible heaters (KHLVA-0502/10 by Omega) had a rectangular shape and consisted of an Inconel etched circuit (25.4 μm thick) encapsulated between two polyimide layers (50.8 μm thick). The heater has a resistance of 80 Ω, and can be supplied with a nominal voltage up to 28 V. It had been successfully used to build an autonomous SMPC actuator (Quadrini et al., 2021), thanks to its low thickness and flexibility.

The polymeric support was made by a commercially available polyethylene terephthalate glycol (PET-G) filament 1.75 mm in diameter.

2.2. Manufacturing and assembling

2.2.1. Shape memory polymer composite hinges

In manufacturing large size solar sails, the use of long SMPC booms would lead to several technical issues. In this view, small-size SMPC hinges, placed only in the folding zones help to overcome most of the issues. The smart hinges have been manufactured according to the procedure shown in Fig. 2. Prepreg stripes, 10×90 mm^2 were cut and SM interlayers, having a mass of 0.2 g which corresponds to a nominal thickness of 150 μm, in the form of an uncured powder were deposited during hand lamination. The chosen SMPCs architecture consisted of three prepreg plies and two SMP interlayers. This architecture represents a good compromise between stiffness, low weight, and recovery load. Two un-cured laminates were placed on a symmetrical aluminum mold, covered with a release film to avoid adhesion during molding.

The mold was obtained by milling, using a CNC machine, by Proxon® equipped with a tool 6 mm in diameter. A 1500 rpm rotational speed and a 0.3 mm depth of pass were selected and the whole tool path was completed in 3 h. The mold, $90 \times 45 \times 12$ mm^3, was designed to give a proper curvature to the smart hinges to compensate residual stresses arising during molding which affects the restoring of the flat configuration upon recovery. The uncured laminates were finally coated with a release film and a 0.2 mm thick aluminum foil to obtain a smooth surface at the end of molding. Cure was lead in oven at 200 °C for 1 h and the consolidation pressure was applied by a crosslinked polyethylene (PEX) thermo-shrinkable tube supplied by Elcon®.

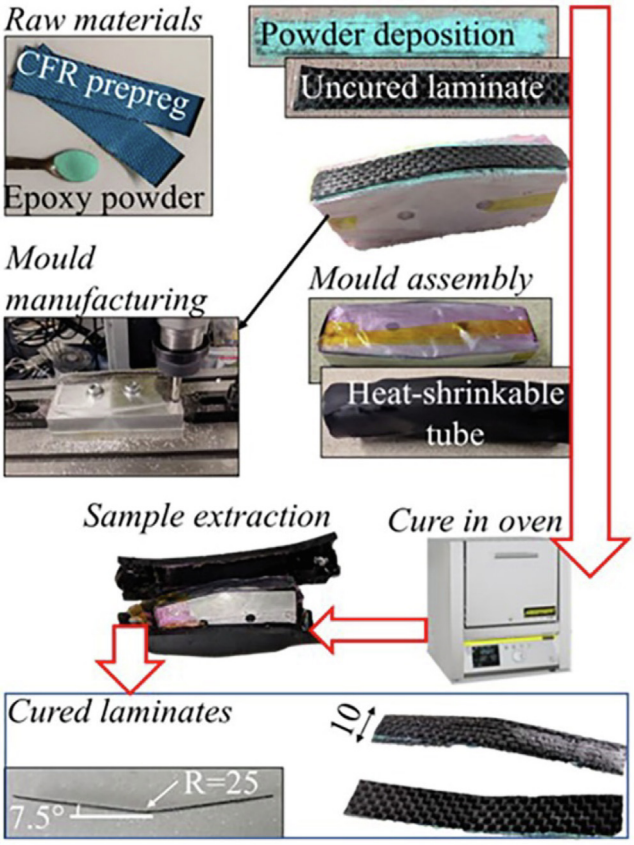

Fig. 2. Manufacturing of the CFR-SMPC hinge.

In the end of manufacturing the SMPC hinges had an average mass and thickness of 1.14 ± 0.04 g and 1.02 ± 0.03 mm respectively. A 25 mm radius of curvature and a residual angle of 15° are clearly visible in Fig. 2. The choice of manufacturing a non-flat laminate is due to the behavior of SMPCs. In fact, SMPCs can be deformed in a temporary configuration through a thermo-mechanical cycle (Quadrini et al., 2019). Moreover, when restoring the undeformed configuration, a little amount of the deformation cannot be recovered. In the case of solar sail, the partial recovery of the deformed SMPC would translate in the partial deployment of the sail, so limiting the efficiency of the interaction with the solar radiation pressure.

The packing of the sail in the minimum allowable volume is ensured by deforming the SMPC hinges in a U-shaped configuration as shown in Fig. 3. The extrados side of the hinge is joined by screw over an aluminum mold produced by milling. The mold has a 4 mm radius of curvature, which prevents hinges failure, and two converging sides downstream of the bending area. Moreover, the mold

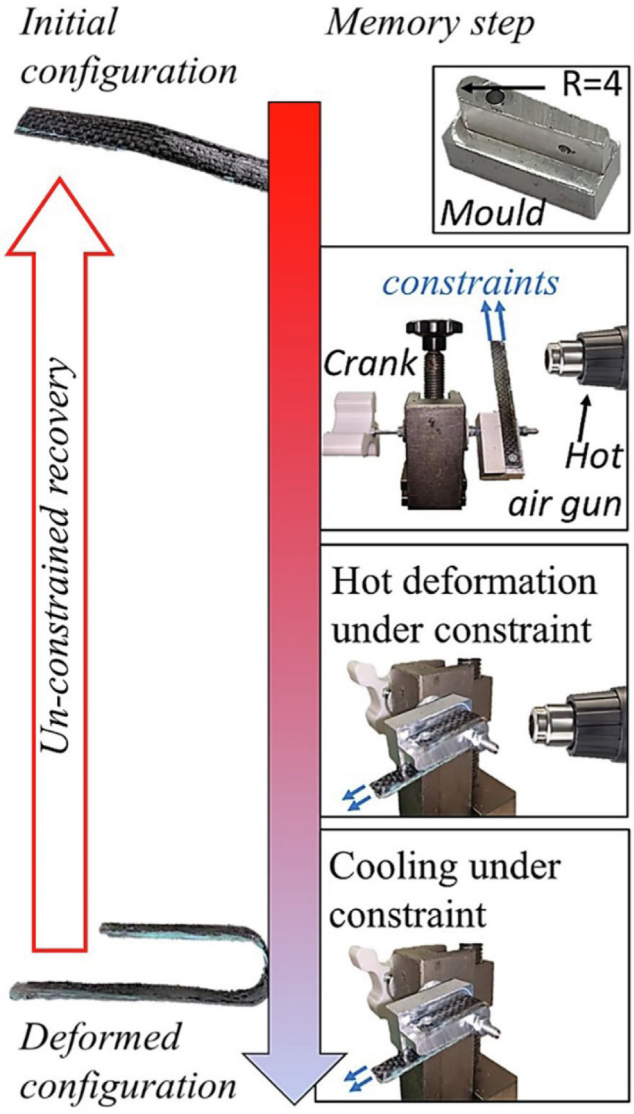

Fig. 3. Memory step procedure for CFR-SMPC hinge deformation.

and a crank are linked with the two opposite edges of an aluminum rod. At the begin of the memory step, the SMPC hinge is pre-heated over the transition temperature and subjected to an external constraint on its free edge. Then, the crank allows the rod rotation and the SMPC hinge is forced to follow the mold profile. Finally, the external constraint is removed once the SMPC hinge is cooled down to room temperature.

This memory system guarantees a uniform deformation of the hinge, which fixes the U-shaped configuration after cooling down to room temperature (T_r). The elastic recovery of the hinge after cooling, is compensated by the convergent sides of the mold, which fix a bending angle of 190°.

2.2.2. CFR frame

The sail frame has been made by 2-ply L-shaped CFR laminates being passive elements. Despite the low number of plies, the boom architecture guarantees the required stiffness for the sail. They were manufactured with the same CFR prepreg used for the SMPC hinges. Cure was performed on a heater plate at 200 °C for 1 h under an applied pressure of 30 KPa. The consolidation pressure was lower compared to the common state of the art, but it was sufficient to ensure good compaction among prepreg plies. In the end of molding, four L-shaped CFR booms were produced, two with nominal dimensions of 125 × 115 mm^2, and two with nominal sizes of 110 × 115 mm^2. The CFR booms had a nominal width of 10 mm and an average thickness of 0.66 mm.

2.2.3. Single body support

The sub-systems shown in Fig. 4 have been produced by additive manufacturing and, in particular by Fused Deposition Modelling through an "Original Prusa i3 MK3". The proposed sub-systems have the role of driving supports and allow the link between passive and active elements. The SMPC hinges can be housed in it. Moreover, the sub-systems ensure continuous contact between SMPC hinge, and the flexible heater placed in the intrados of the smart hinge. Finally, they were designed to avoid deployable angle higher than 180°. In this way the SMPC hinge recovery is fixed in the flat open configuration and the unrecovered deformation is able to develop a load which keep in tension the sail membrane.

The support was designed to overcome some criticalities due to manufacturing. In the design phase, the support geometry was chosen in such a way to develop a model able to be printed in one step as a single body with the minimum amount of supports. The conceptualization of the support geometry is shown in Fig. 4. The first model consisted of two wings linked by a rotoidal kinematics. The rotoidal kinematics consisted of a pivot coupled with two rings respectively provided at the edges of the two wings. The 180° open configuration was fixed when the contact of the two wings is reached. Apart small optimization of the proposed layout, the need of locating elsewhere the volume of the coupling area as well as the lack of a joint area led to the development of a more efficient solution. It consisted of a central body with two holes allowing the coupling with two rectangular wings. The wings have a narrowed section on the one edge ending with a cylindrical pivot. Moreover, equally spaced holes, 2 mm in diameter, are located on each wing along their longitudinal axis to allow coupling with the frame and with the SMPC hinge. Lighteners are also provided on the wings to allow housing of an insulating layer to prevent degradation of the polymeric hinge upon SMPC heating. Relative motion between the wings and the central body was ensured. A pin was obtained on the pivot of the wings. The locking of the wings in the flat open configuration is guaranteed when the pin comes into contact with the central body of the support as shown in the A-A section of Fig. 4. The nominal sizes of the support in the open configuration were 100 × 10 × 6 mm^3, whereas in the closed configuration were 50 × 10 × 25 mm^3. The

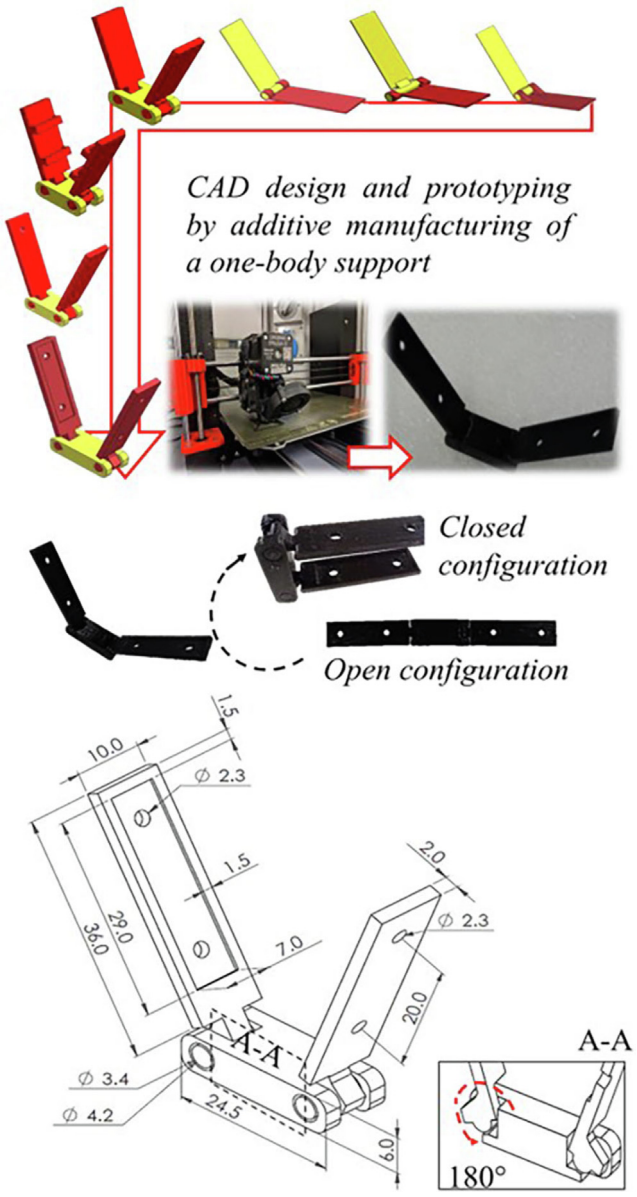

Fig. 4. CAD-design and FDM-manufacturing of the one-body support.

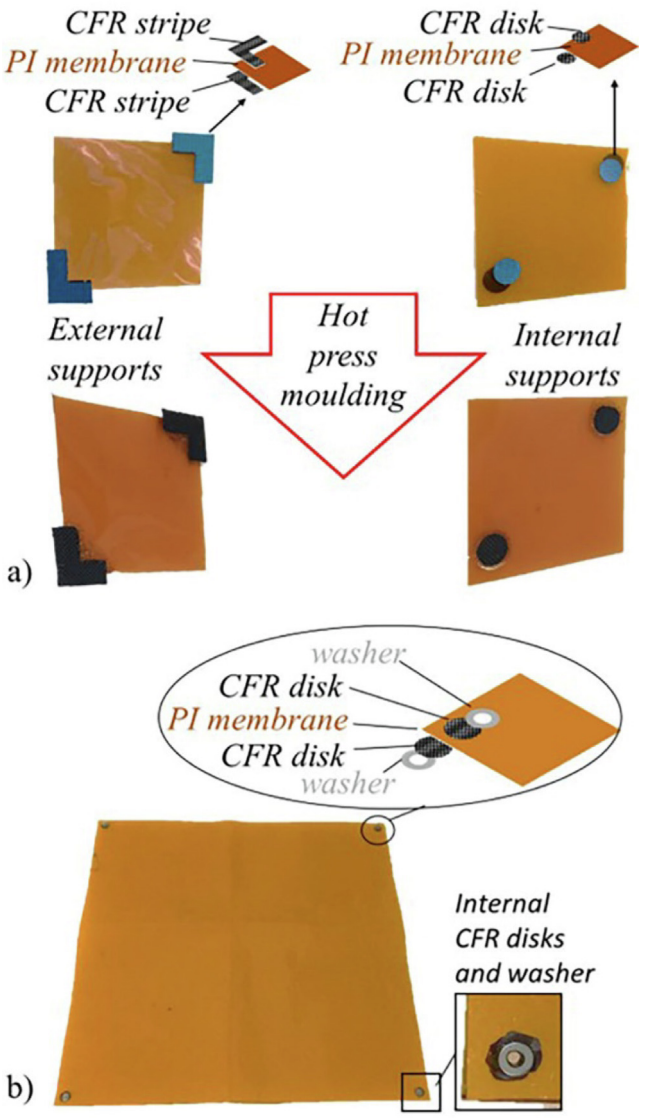

Fig. 5. Joints between CFR composite and Polyimide film: (a) Two different configurations of CFR supports; (b) Final configuration made of internal CFR disks with steel washers.

devices have an average mass of 2.61 g, resulting from 10 % filling during 3D printing. Polymeric support is not the best solution to withstand severe thermal cycles but are helpful in understanding the major issues concerning the right assembly of the novel sail architecture.

2.2.4. Sail joining

The joint between the membrane and the frame is another challenge in the manufacturing of large solar sails. The Kapton membrane was initially provided with 2-ply CFR supports placed on two opposite vertexes as shown in Fig. 5a. Compression molding on a heater plate at 200 °C for 1 h under an applied pressure of 70 kPa ensured the adhesion of the supports to the membrane.

Two different configurations for the CFR supports have been chosen. The first configuration consisted of external CFR supports partially overlapped on the sail membrane corner. The supports surface was 1500 mm^2 on average and the overlapped area was of about 650 mm^2. The second configuration consisted of internal CFR disks, 25.4 mm in diameter placed on both the surfaces of the polyimide film. Preliminary investigations on these configurations aimed at developing the optimal solution shown in Fig. 5b. Steel washers, 3 mm as external diameter were compression molding on the CFR disks. Holes of 2 mm in diameter were also machined to use connecting wires. The adopted washer avoided tearing of the CFR supports when in operation. In all the manufactured solutions, wrinkles are present around the CFR supports because of the resin bleeding during molding.

2.2.5. Solar sail prototype

The final prototype of the small deployable sail is shown in Fig. 6. The polymeric supports are placed in the middle

of the frame sides. Moreover, each support links two adjacent CFR L-shaped booms and screws have been used for joining. The SMPC hinges are housed in the polymeric supports (Fig. 6). One edge of the SMPC hinge was also joined by screw with the polymeric support. The flexible heater and both edges of the SMPC hinges were also constrained through Kapton stripes. In this way, continuous contact between the flexible heater and the SMPC hinges as well as the sliding of the heater onto the same hinges during the recovery step is ensured. Moreover, the same Kapton stripes also allowed the sliding of the SMPC free edges onto the polymeric support during the deployment step. The prototype has a mass of 60 g considering the heaters and the wiring, a nominal surface area of 260 × 260 mm^2 and an areal density of 0.09 g/cm^2.

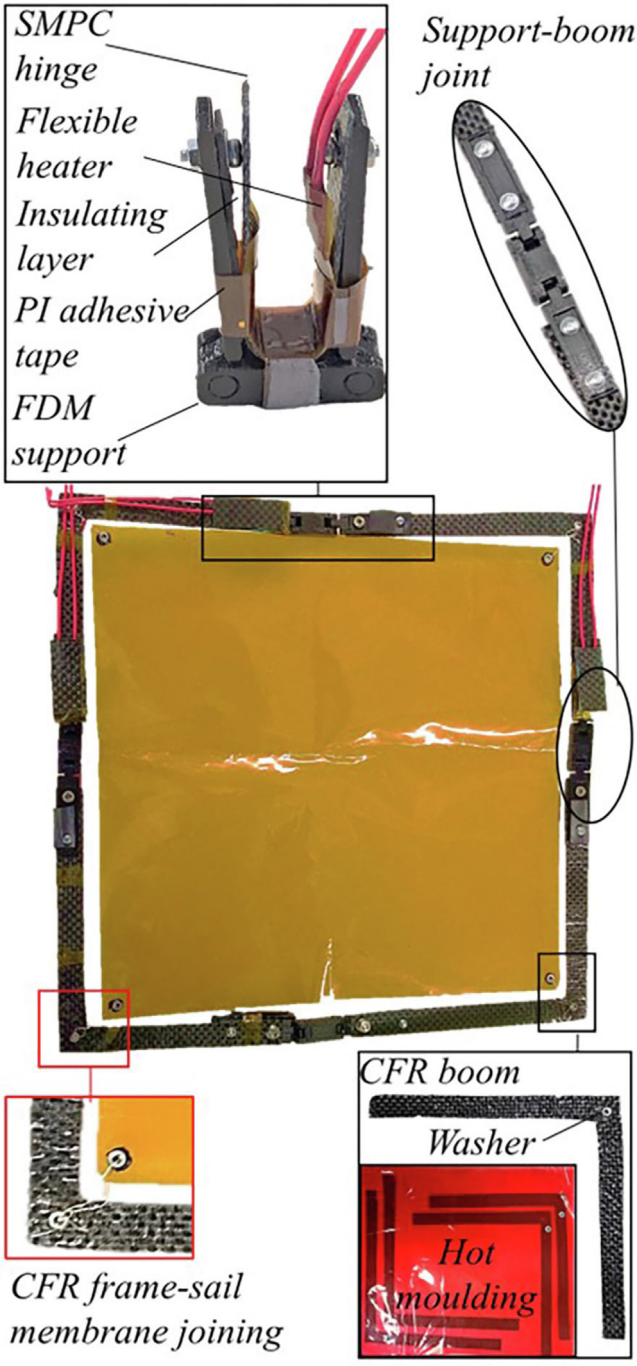

Fig. 6. Final configuration of the small-scale solar sail.

2.3. Testing

Deployment of the solar sail prototype mainly depends on the actuation load exerted by the SMPC hinges upon recovery. In addition, the joining of the sail membrane with the CFR frame should prevent the rise of tears during operation. Moreover, the right design of the packing strategy is required to avoid interference of the sail membrane upon deployment.

2.3.1. Temperature measurement

The thermoset SMPs and SMPCs can be deformed in the temporary configuration if the glass transition temperature T_g is reached and exceeded. In fact, over this temperature, the molecular mobility is high and large deformation can be applied to the SMPCs without any damages. Under constrained cooling, most of the applied deformation can be stored and the temporary configuration becomes stable. When heated again without any constraints over the T_g, molecular mobility increases and the SMPCs can restore the undeformed configuration.

In the current study, heating is obtained by flexible heaters fixed on the surface of the SMPC hinges. Heaters are powered by an external unit and the recorded temperature is function of the applied voltage. The right operation of the SMPCs is obtained if the glass transition temperature is exceeded on the whole laminate. Temperature evolution has been recorded by 2 k-type thermocouples placed on the top and on the bottom of a SMPC as shown in Fig. 7. The whole heating–cooling cycle was recorded for the applied voltage of 26 V. The heater, placed on the top of the laminate, covered the thermocouple and higher temperature values were so recorded with a maximum gradient of about 70 °C at the equilibrium. Only one heater was used for

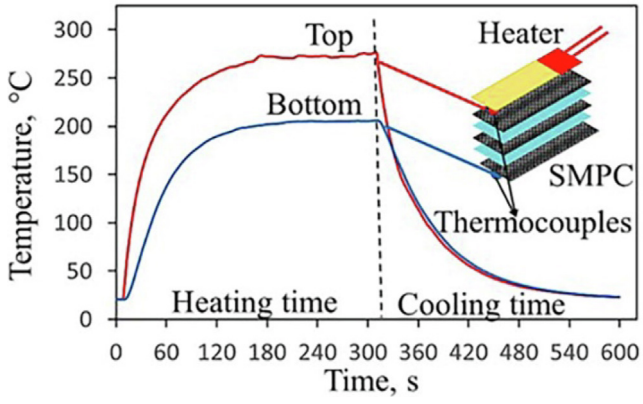

Fig. 7. Temperature curves of the SMPC hinge at the maximum applied voltage of 26 V.

SMPC recovery as it allowed the whole recovery of the hinges so limiting the required power consumption which instead would increase in case of a second heater placed on the extrados. In the future, a thermal envelope (e.g. MLI) will be a valuable solution to equalize the temperature on both sides of the hinges. Moreover, MISSE 9 experimentation revealed the absence of decomposition or pyrolysis of the SMPC (Santo et al., 2024) in LEO environment, under solar radiation. Furthermore, on the raw constituents of the flexible heater (an etched copper circuit between two polyimide films) decomposition or pyrolysis have never been observed also at high voltages. During cooling, the temperature gradient disappeared in less than 1 min. Voltages ranged between 18 V and 26 V (Fig. 8) at step increment of 2 V. Lower values were not able to set the T_g all over the manufactured laminate whereas higher voltages were responsible of heater degradation.

In all testing condition temperature plateau upon heating was reached in about 3 min. Moreover, temperature gradient reduces to 47 °C with the lowest applied voltage.

2.3.2. Mechanical testing

The actuation load of the SMPC hinges upon recovery (Fig. 9a) and the strength of the adhesion between the CFR supports and the sail membrane (Fig. 9b) were measured by recovery load and tensile tests respectively. Tests were performed on an MTS Insight 5 Universal testing machine. The recovery load tests were carried out using an indenter with a 2 mm tip coupled with a 2 mm hole on the deformed SMPC hinge. This configuration prevented sliding of the hinges when heated through the flexible heater. The recovery load was recorded for applied voltages ranging between 18 V and 26 V, with steps of 2 V. Tensile tests were carried out at 1 mm/min up to failure.

2.3.3. Folding strategies and shape memory testing

The folding of huge deployable structures before their launch on orbit is still a hard task and different strategies are under evaluation. The same technical issues can be proposed also at lab-scale. For the manufactured solar sail prototype, a hierarchical deployment strategy was implemented. To avoid superimposition of the Kapton film a two-step unfolding procedure is required. The first couple of two opposite sides of the frame would deploy while the residual couple would remain fixed. When the deployment of the first two sides ends, deployment of the residual sides can start. A CAD model of the proposed strategy is shown in Fig. 10a) and the experimental validation is shown in Fig. 10b).

In this way the minimum packed volume is obtained, and the height of the folded structure is mainly function of the polymeric support base. Fig. 10a) also highlights that one of the polymeric supports is reverted to have the same configuration of the support on the opposite side after the first level of deployment. The two-step deployment proce-

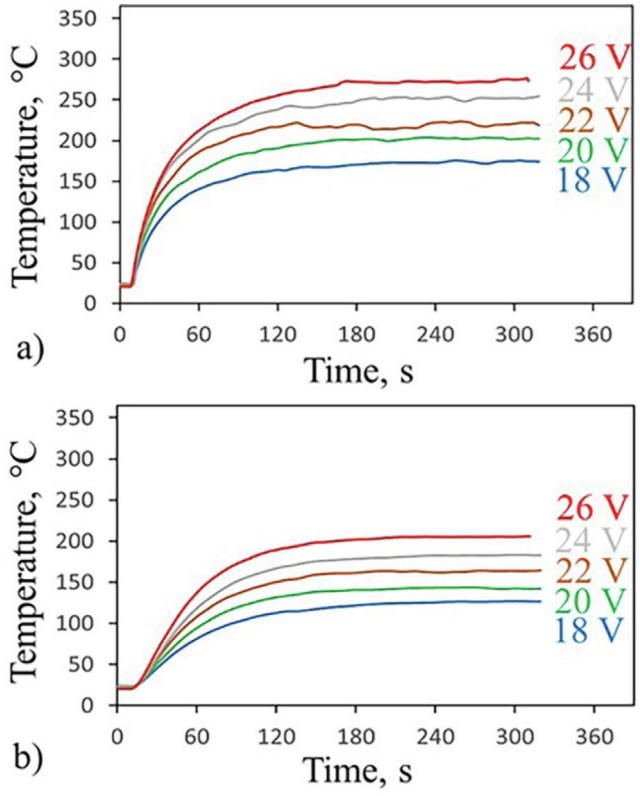

Fig. 8. Heating curves at different applied voltages. (a) Heating curves recorded at the top of the SMPC laminate; (b) Heating curves recorded at the bottom of the SMPC laminate.

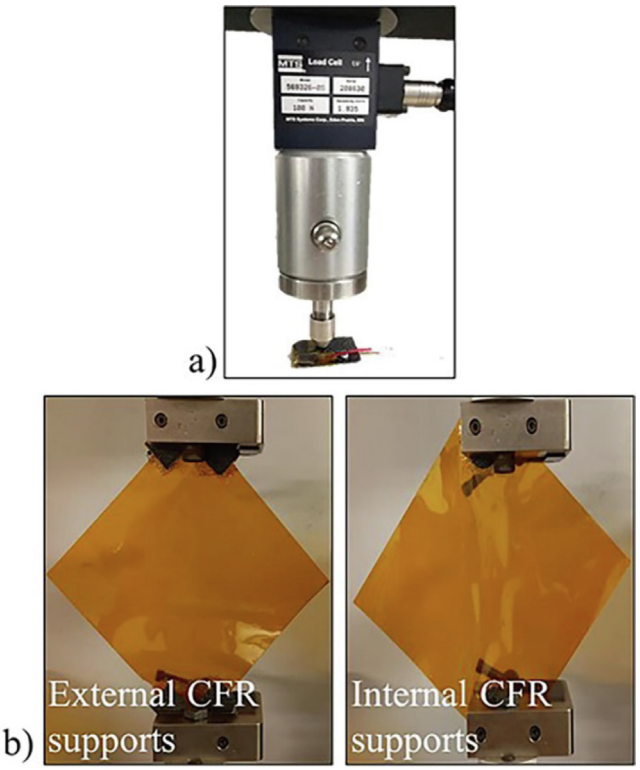

Fig. 9. a) Recovery load testing setup, b) Testing setup to evaluate the adhesion of the CFR eyelet onto the sail membrane.

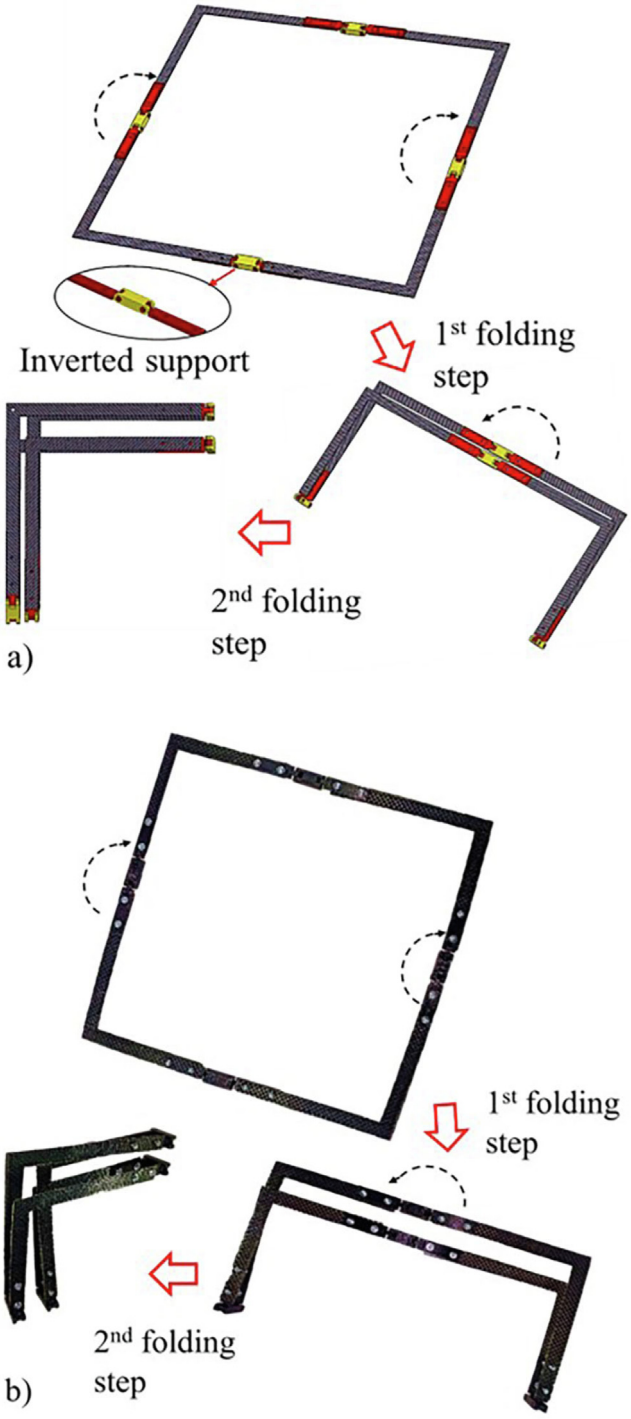

Fig. 10. Analysis of a two-step folding strategy: (a) CAD-design of the folding strategy; (b) Validation with the small-scale CFR frame.

dure can be reverted to pack the structure in the minimum allowable volume as shown in Fig. 11. Interference of the sail membrane is prevented and contact with the flexible heaters is also avoided.

The packed prototype has the shape of a square based parallelepiped with 135 mm side and 26 mm in height being the base length of the polymeric support. The proposed

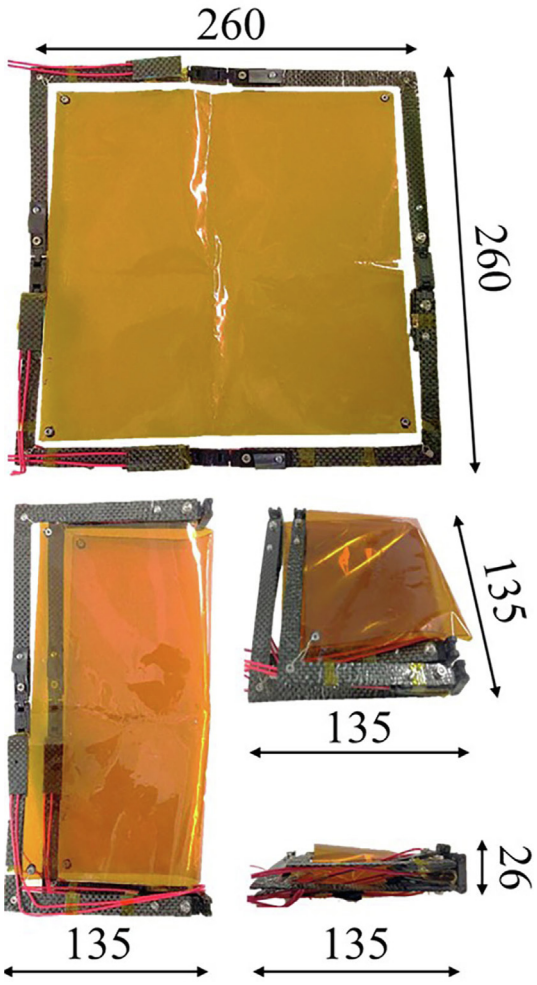

Fig. 11. Two-step folding for the small size sail.

folding strategy leads to a surface reduction of 48 % and 73 % after the first and the second level of packing respectively.

In the shape memory tests, the flexible heaters were powered by an external unit (Fig. 12a).

Flexible heaters on two opposite sides of the prototype were connected in parallel. A two button-switch manages the hierarchical deployment of the small sail. Shape memory tests on the whole prototype were carried out in two different layouts as shown in Fig. 12b. The maximum tension of 26 V was applied for both layout configurations whereas an additional test at 25 V was performed for the "layout 2" configuration.

3. Results

3.1. SMPC hinge testing

Results from the recovery load tests are shown in Fig. 13 as load over time at a fixed applied voltage. The applied voltages ranged from 18 V to 26 V with 2 V as a step increment. Consequently, the required nominal power for the

flexible heater ranged from 4.0 W to 8.4 W. At the beginning of the test, load increases linearly up to a peak load before 1 min of testing. The peak load rapidly decreases and a further increase of the load up to a plateau value, lower than the peak load, is finally obtained. Designing of the SMPC hinge strongly depends on the value of the plateau load. The maximum peak load (0.94 N) is obtained for the maximum applied voltage (26 V). The plateau values are recorded after 3 min of heating confirming data of the temperature evolution measurements. The recorded values are comparable, ranging from 0.78 N to 0.84 N with an average value of 0.81 N. Once the plateau value is reached, the hinge is left under cooling and the load decreases down to zero following a curve where two different regions can be identified. In the first region the load follows a non-linear decrease whereas in the second region it decreases linearly.

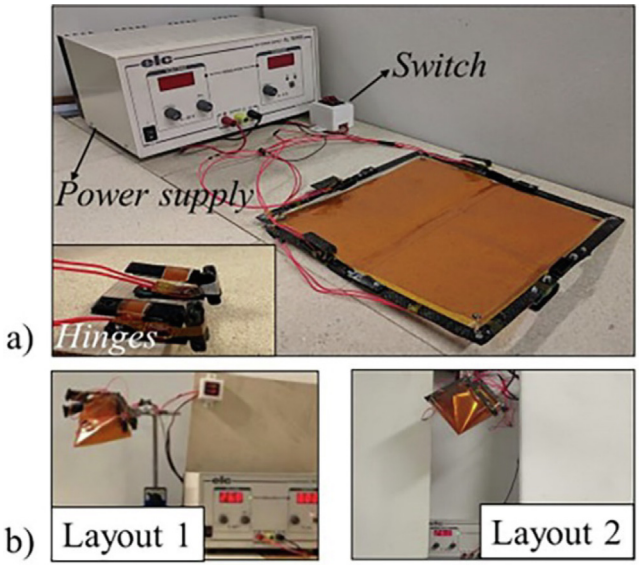

Fig. 12. Shape recovery of the small size solar sail: (a) Testing setup configuration; (b) Layouts for the shape recovery analysis of the sail prototype.

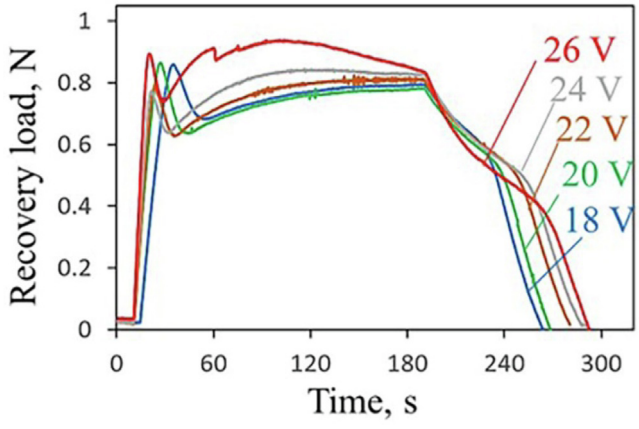

Fig. 13. Recovery load under constraint of the SMPC hinge at different applied voltages.

Curves have the same slope during the cooling stage whereas upon heating the slope increases by increasing the applied voltage because of the higher heating rate of the SMPCs.

3.2. Polyimide-CFR joint testing

Results of tensile tests for CFR-sail membrane joining strength are shown in Fig. 14. The internal CFR supports configuration has a higher value of the ultimate tensile load, about 580 N whereas the external CFR supports configuration joint exhibited an ultimate tensile load of about 226 N. The failure is due to tears developing in the sail membrane very close to the joints.

The external CFR supports configuration is more suitable to join the sail body with the CFR frame, being completely overlapped over the sail membrane. On the other side, the external CFR supports configuration is partially overlapped on the sail membrane thus inducing thickness variations which compromise the strength of the solution. Moreover, "Sharp edges" are present in the case of external CFR supports and this led to stress intensification. The internal CFR supports have been used together with metallic washers to ensure CFR frame-sail membrane linking through thin iron wires. The lack of metallic washers would induce tearing of the CFR disks when tensioned by the linking wire.

3.3. Shape recovery tests

The recovery tests on the prototyped modular solar sail by using flexible heaters confirmed the potential of the SMPC hinges. The recovery rate depends by the heating systems and fully recovery can always be obtained apart small residual angles due to the stiffness of the sail membrane. The shape recovery of the adopted assembly is shown in Fig. 15. Two assemblies are connected in parallel to replicate the recovery hierarchical deployment of the

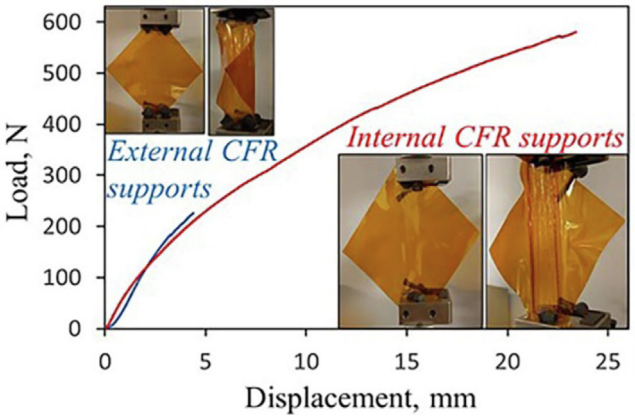

Fig. 14. Load-displacement curves for testing the Polyimide-CFR joint adhesion.

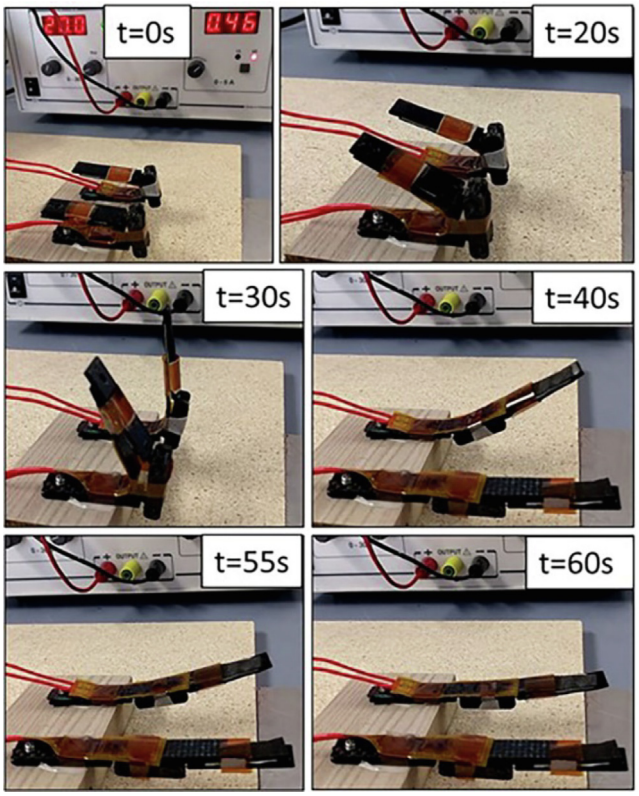

Fig. 15. Shape recovery of two polymeric support-SMPC hinge-assemblies.

solar sail prototype. The system was powered with a tension of 20 V, corresponding to a power of 9.2 W.

Full recovery was obtained, even if not at the same time. In fact, 40 s and 60 s were the recovery time of the two assemblies, with an average angular recovery speed of about 4.5 deg/s and 3.0 deg/s respectively for the assembly furthest and closest to the external power supply. The different recovery time is influenced by factors, such as the friction between the elements of the polymeric support or the wiring between the flexible heaters and the unit power supply. Moreover, the adopted insulating solution for the heater-SMPC hinge-polymeric support assembly, avoided melting of the supporting device itself. In view of future developments, the polymeric supports would be replaced by light metallic sub-systems minimizing the thermal dissipation by proper design so eliminating the need of proper insulating layers.

Full deployment of the solar sail prototype has been reached for the proposed test configurations. In both layout configurations, the solar sail is constrained in one of the corners. In the layout 1 (Fig. 16) all the rotational and translational degrees of freedom are locked whereas in layout 2 (Fig. 17) the rotation around the axis orthogonal to the plane of the membrane is free. The designed hierarchical deployment is clearly visible, and no interferences of the sail membrane occurred upon unfolding. The applied voltage was 26 V, corresponding to a power of 15.3 W (due to parallel connection) so maximizing the

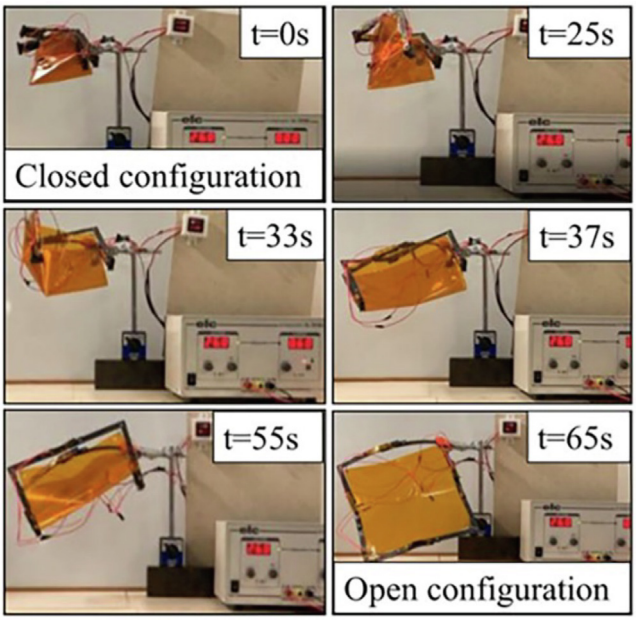

Fig. 16. Sail deployment sequence in the layout 1 configuration.

recovery speed and the recovery load exerted by the SMPC hinges. The first level of deployment required about 55 s and 65 s respectively for the layout 1 and layout 2, with an average angular recovery speed of 3.3 deg/s and 2.8 deg/s respectively. The second level of deployment required about 10 s and 30 s with an average angular recovery speed of 18 deg/s and 6 deg/s respectively.

For the layout 2 a further test at 25 V was performed. The recovery time was about 140 s for the first level of deployment and 50 s for the second one. The first level of deployment took more time because of some wrinkles arising on the sail membrane. This was the result of several tests which affected the integrity of the sail body. This issue can be easily overcome because the commonly adopted sail membranes has significantly lower thickness compared to the commercial Polyimide film used in the current experimentation.

4. Discussion

Solar sail technology still lacks consolidated technological developments. Several issues must be solved, from manufacturing to folding and deployable solutions. Shape memory polymer composites are a potential and viable innovative solution to match most of these requirements. They result as the optimal synthesis between the structural properties of traditional composite laminates and the functionalities of the SMPs. Their low weight and process using the same manufacturing technologies of traditional laminates are additional advantages. Moreover, their high deformation capabilities allow to define efficient folding strategies, and the actuation load exerted upon recovery ensures deployment of the folded architecture. Several steps are required to design and validate the new concept

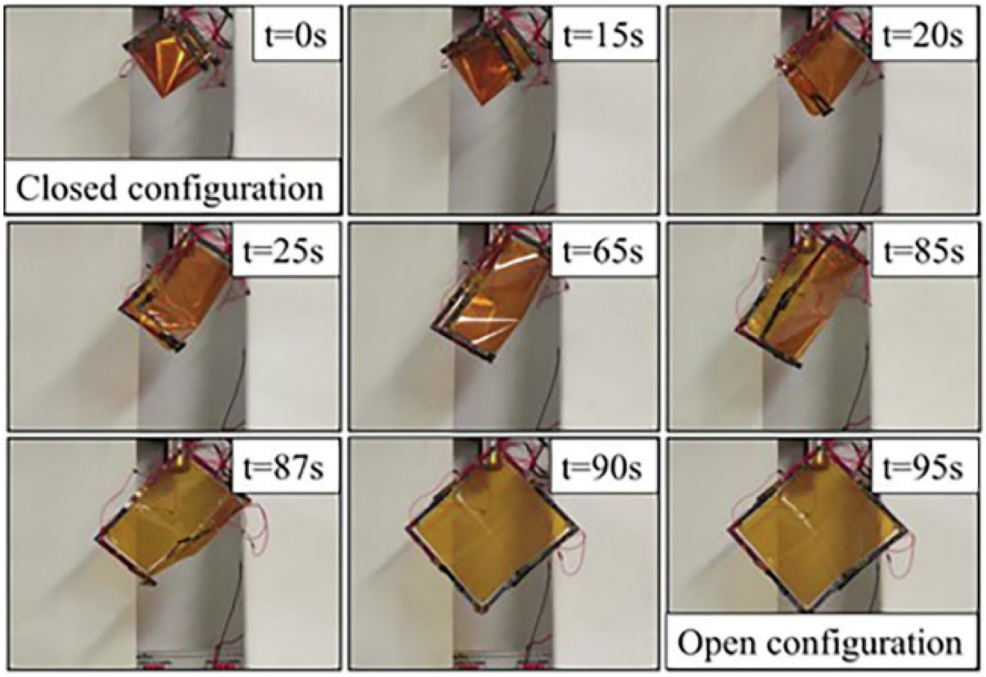

Fig. 17. Sail deployment sequence in the layout 2 configuration.

of solar sails based on the use of SMPCs because of their non-conventional behavior. Differently from other solar sail developed prototype (Santo et al., 2019), the proposed small-scale solution is based on a modular architecture. Compression molding gives the required consolidation pressure both for the flat 2-ply L-shaped CFR booms and for the bent SMPC hinges where an OOA process has been used. SMPC hinge with 3-CFR ply and 2 SMP interlayers was the optimal architecture able to combine the requirements of low weight, high deformation capabilities and actuation load for sail deployment. SMPC hinge activated by flexible heaters exceeded the glass transition temperature for all the applied voltages. The actuation load showed a maximum of 0.94 N and 0.84 N respectively in terms of peak load and plateau load for the maximum applied voltage of 26 V. The minimum obtained values were of 0.82 N as peak load for the applied voltage of 22 V and 0.78 N as plateau load for the applied voltage of 20 V (Table 1). The actuation load is the plateau load of the test and is used for hinge designing.

Despite the low recorded values, even in the worst case the plateau load is sufficient to overcome the weight of the sail. The additional load is suitable to overcome friction of the polymeric single body printed supports and the wrinkles arising in the sail membrane upon deployment. The difference of the recorded recovery loads is less than 10 % meaning that the applied voltage, either, heating, does not have influence on the actuation load if the transition temperature of 120 °C (Quadrini et al., 2019) is exceeded. Instead, the actuation load is only dependent by the adopted SMPC architecture and the applied deformation.

Table 1
Measured data from temperature and recovery load tests.

	SMPC hinge				
	18 V	*20 V*	*22 V*	*24 V*	*26 V*
Top temperature, °C	174.3	202.4	221.0	251.8	269.6
Bottom temperature, °C	126.7	143.0	163.3	182.6	205.2
Temperature gradient, °C	47.6	59.3	57.7	69.1	64.5
Peak load, N	0.86	0.87	0.82	0.85	0.94
Plateau load, N	0.80	0.78	0.81	0.83	0.84

For the first time, additional sub-systems, in the form of hinges, have been prototyped with the aim of driving the SMPC recovery toward the nominal flat required configuration. The SMPC hinges were produced in a bent configuration to overcome the residual stresses developing during manufacturing and affecting the restoring of the undeformed configuration. Moreover, the initial imposed curvature has been chosen to allow a recovery angle higher than 180°. In this way the polymeric support can fix the SMPC recovery to the flat configuration and the unrecovered deformation is responsible of a residual load which keep the sail membrane in tension. In this way interaction with the solar radiation pressure is maximized. Moreover, the adopted sub-systems are the joining element between the active SMPC hinge and the passive CFR booms. In the optic of future developments, the substructures would be made by metal alloy to avoid degradation of the polymers due to atomic oxygen and melting due to the conductive heat flow generated by the heaters if proper insulating strategies are not implemented. Geometrical optimization and the choice of the suitable material for the supports are the successive challenges to face.

Table 2
Data measured from shape recovery tests.

	Small size solar sail			
	Recovery time, s		*Average angular recovery speed, deg/s*	
	1^{ST} unfolding step	2^{ND} unfolding step	1^{ST} unfolding step	2^{ND} unfolding step
Layout 1	55	10	3.3	18
Layout 2	65	30	2.8	6

The frame-sail membrane joining has been obtained by wires, linking two supports made of CFR disks and metallic washers placed on the membrane with two metallic washers placed on the corner of the CFR booms. Washers have been compression molding on the corners of the frame whereas the assembly CFR disk-metallic washer has been compression molding on the membrane corners. The use of washers prevented composite tearing if the structure undergoes to severe stretch condition. Results from tensile tests revealed the rise of wrinkles before failure and highlighted the soundness of the eyelet solution. In fact, the polyimide membrane with internal CFR disks exhibited a failure load of 580 N, about 156.9 MPa extracted considering an ideal section following the evolution line of tearing. The failure load for the external CFR stripes partially embedded the sail membrane was 226 N, about 64.1 MPa with a load and stress decrease of 61 % and 59 % respectively compared to the former configuration. The internal CFR supports configuration minimizes wrinkles due to resin bleeding arising during compression molding. True solar sail membranes are made by a 3 μm thick CP1 with a nanometric aluminized coating to increase the surface reflectivity. Limiting the areas with stress intensification as the ones obtained by resin bleeding is fundamental to preserve the integrity of the sail body. The sail membrane was smaller (230×230 mm^2) than the frame to avoid interference with the hinge-polymeric support-heater assembly during folding and unfolding steps.

The conceptualized hierarchical strategy of deployment has been implemented. A couple of hinges connected in parallel at a time have been activated thus obtaining two levels of unfolding. In the proposed shape memory testing layout configurations, full deployment was obtained in less than 2 min for the applied voltage of 26 V. Tests revealed that decrease of the degrees of freedom translates into a decrease of the recovery time as shown in Table 2. In fact, in the layout 1 where no degrees of freedom are allowed at the constrained corner, the recovery time is 65 s, and it increases up to 46 % when considering the layout 2.

Moreover, the first unfolding step is longer than the second one. This occurrence depends by the higher amount of mass that the first couple of SMPC hinges have to move. A reduction of 82 % and 54 % between the first and the second unfolding step has been observed respectively for the layout 1 and layout 2. Consequently, the average angular recovery speed doubled for the layout 2 and increased up to six times for the layout 1. Small residual angles still remain after deployment due to wrinkles of the membrane which counter-act the recovery of the SMPC hinges. Minimizing recovery time is not a stringent task for deployment of large solar sails. Membrane tearing could occur due to the high developed level of stress. The proposed SMPC hinge has been designed for solar sails, but the current architecture of the sail deployment is closer to the case of drag sails, because of the small size of the prototyped sail. For drag sails of CubeSats, the final configuration of the deploying mechanism is already valid. In particular, for each unfolding step, two hinges are required and consequently two heaters must be powered. In the worst case (26 V) the power requirement is around 15.3 W, which can be supplied by the Cubesat batteries. In case of solar sails, very large and light structures are necessary and additional constraints are present for the hinge weight. Even if solar exposure may be used for SMPC actuation, the current idea is continuing to use electric supply also for solar sails. In that case, most of the weight is associated with wiring. Nevertheless, one of the possible architectures for solar sails uses a large electrochromic membrane (Mu et al., 2015), because of the need of sail maneuvering, and the same problem of wiring and electric supplying is present. In this view, SMPC hinges would be integrated in those architectures, taking advantages by the wiring and supplying of the electrochromic membrane. Finally, heating coming from solar radiation could affect the established deployment hierarchy. For this reason, the adopted heating system must be proper integrated.

The proposed frame architecture allows performing on Earth testing with wider sail prototypes, but the polymeric support geometry must be optimized and minimized if multiple folding steps are implemented. In fact, wide supporting sub-structures severely affected the final minimum packed sail volume.

5. Conclusions

In this work a novel architecture of a smart solar sail prototype with SMPC hinges and CFR booms has been manufactured and tested on Earth. Small size architectures are the only means to investigate all the issues related to the operation of real solar sails. Their weights can overcome the recovery loads of the adopted actuation systems so affecting free deployment. Despite that, the design and the obtained results are promising for a future implementation of drag sail in the field of debris mitigation. Deployment of the developed prototype has been obtained using

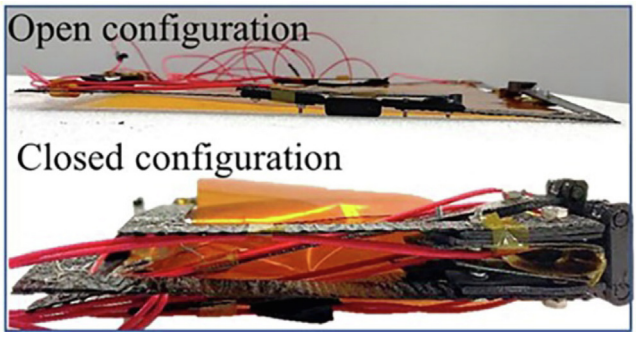

Fig. 18. Small size solar sail in the open and closed planar configuration.

SMPC as hinges. The optimal structure (three CFR plies and two SMP interlayers) has been found and the consolidated innovative OOA process allowed co-curing of the two epoxy systems, (the one of the prepreg and the one of the SM resin) and the required consolidation was also obtained. SM properties of the hinges were activated by heating supplied through flexible heaters. The measured recovery loads were sufficient to compensate the weight of the whole prototype as well as the additional forces due to the polymeric sub-systems. These additional devices ensured not only the joining between the SMPC hinges, the CFR booms, and the flexible heaters but they also drive the hinges recovery toward the flat planar configuration as shown in Fig. 18.

Criticalities arising from warpages due to membrane embedding in the solar sail frame have been overcome by using properly designed eyelet junctions. In this way the efficiency of the interaction between the sail membrane with the solar radiation pressure is not affected and the areas with stress intensification are strongly reduced.

Full hierarchical deployment has been obtained in the proposed shape memory tests and recovery time could be modulated by varying the applied voltage.

Finally, some important findings have been obtained, from manufacturing, to sail folding and unfolding strategy to the autonomous heating system. Commercially available materials already validated in harsh space environment as well as robust and innovative manufacturing technology is scalable for higher sizes. Different steps are still under evaluation as the optimization of the supporting devices, and the constraint of the heating devices with the SMPC hinges. In this view, embedded flexible heaters seems to be the most efficient solution. The performed experiments provided several information which can be used to numerically simulate the operation of large solar sail in space environment.

Declaration of competing interest

The authors declare that they have no known competing financial interests or personal relationships that could have appeared to influence the work reported in this paper.

Acknowledgements

This work is performed jointly under the Implementing Agreement between the Italian Space Agency and DIAEE – Sapienza University of Rome n. 2019-28-HH.0 - CUP n. F84I19001070005 related to R&D activities on solar photonic propulsion. The Implementing Agreement is based on the Framework Agreement between ASI and "La Sapienza" n. 2015-1-Q.0. Moreover, the authors are grateful to Dr Fabrizio Betti and Dr. Daniele Ippoliti for the support given in the experimentation.

References

Bassetto, M., Niccolai, L., Boni, L., Mengali, G., Quarta, A.A., Circi, C., Pizzurro, S., Pizzarelli, M., Pellegrini, R.C., Cavallini, E., 2022. Sliding mode control for attitude maneuvers of Helianthus solar sail. Acta Astronaut. 198, 100–110. https://doi.org/10.1016/j.actaastro.2022.05.043.

Bellisario, D., Quadrini, F., Iorio, L., Santo, L., Zhang, Z., Li, X., Dong, H., Semitekolos, D., Konstantopoulos, G., Charitidis, C.A., 2022. Microscopic testing of carbon fiber laminates with shape memory epoxy interlayer. Mater. Today Commun. 32103854. https://doi.org/10.1016/j.mtcomm.2022.103854.

Bellisario, D., Iorio, L., Proietti, A., Quadrini, F., Santo, L., 2023. Out-of-autoclave molding of carbon fiber composites pipes with interlaminar carbon nanotubes. In: In Proceedings of the 26th International Esaform Conference on Material Forming Krakow. https://doi.org/10.21741/9781644902479-194.

Boschetto, A., Bottini, L., Costanza, G., Tata, M.E., 2019. Shape memory activated self-deployable solar sails: small-scale prototypes manufacturing and planarity analysis by 3D laser scanner. Actuators 8 (38), 1–10. https://doi.org/10.3390/act8020038.

Bovesecchi, G., Corasaniti, S., Costanza, G., Tata, M.E., 2019. A novel self-deployable solar sail system activated by shape memory alloys. Aerospace 6 (78), 1–11. https://doi.org/10.3390/aerospace6070078.

Dang, X., Feng, F., Plucinsky, P., James, R.D., Duan, H., Wang, J., 2022. Inverse design of deployable origami structures that ap-proximate a general surface. Int. J. Solids Struct. 234-235, art. no. 111224. doi: 10.1016/j.ijsolstr.2021.111224.

Fernandez, J.M., Lappas, V.J., Daton-Lovett, A.J., 2011. Completely stripped solar sail concept using bi-stable reeled composite booms. Acta Astronaut. 69 (1–2), 78–85. https://doi.org/10.1016/j.actaastro.2011.02.015.

Fu, B., Sperber, E., Eke, F., 2016. Solar sail technology-A state of the art review. Prog. Aerosp. Sci. 86, 1–19. https://doi.org/10.1016/j.paerosci.2016.07.001.

Genta, G., Brusa, E., 1999. The parachute sail with hydrostatic beam: a new concept for solar sailing. Acta Astronaut. 44, 133–140. https://doi.org/10.1016/S0094-5765(99)00039-9.

Grundmann, J.T., Bauer, W., Biele, J., et al., 2019. Capabilities of GOSSAMER-1 derived small spacecraft solar sails carrying MASCOT-derived nanolanders for in-situ surveying of NEAs. Acta Astronaut. 156, 330–362. https://doi.org/10.1016/j.actaastro.2018.03.019.

Hibbert, L.T., Jordaan, H.W., 2021. Considerations in the design and deployment of flexible booms for a solar sail. Adv. Space Res. 67 (9), 2716–2726. https://doi.org/10.1016/j.asr.2020.01.019.

Johnson, L., Young, R., Montgomery, E., Alhorn, D., 2011. Status of solar sail technology within NASA. Adv. Space Res. 48 (11), 1687–1694. https://doi.org/10.1016/j.asr.2010.12.011.

Kezerashvili, V.Y., Kezerashvili, R.Y., 2021. On deployment of solar sail with superconducting current-carrying wire. Acta Astronaut. 189, 196–198. https://doi.org/10.1016/j.actaastro.2021.08.018.

Kezerashvili, V.Y., Kezerashvili, R.Y., 2022. Solar sail with superconducting circular current-carrying wire. Adv. Space Res. 69 (1), 664–676. https://doi.org/10.1016/j.asr.2021.10.052. 7.

Kezerashvili, V.Y., Kezerashvili, R.Y., Starinova, O.L., 2023. Solar sail with inflatable toroidal shell. Acta Astronaut. 202, 17–25. https://doi.org/10.1016/j.actaastro.2022.09.039.

Kezerashvili, V.Y., Kezerashvili, R.Y., 2024. Theoretical approach to circular solar sail deployment. Adv. Space Res. 73, 4731–4741. https://doi.org/10.1016/j.asr.2024.02.002.

Kezerashvili, R.Y., Starinova, O.L., Chekashov, A.S., Slocki, D.J., 2021. A torus-shaped solar sail accelerated via thermal desorption of coating. Adv. Space Res. 67, 2577–2588. https://doi.org/10.1016/j.asr.2020.06.041.

Li, F.F., Liu, L.W., Lan, X., Zhou, X.J., Bian, W.F., Liu, Y.J., Leng, J.S., 2016. Preliminary design and analysis of a cubic deployable support structure based on shape memory polymer composite. Int. J. Smart Nano Mater. 7 (2), 106–118. https://doi.org/10.1080/19475411.2016.1212948.

Liu, Y.J., Du, H.Y., Liu, L.W., Leng, J.S., 2014. Shape memory polymers and their composites in aerospace applications: A review. Smart Mater. Struct. 23 (2). https://doi.org/10.1088/0964-1726/23/2/023001, art no 023001.

Liu, J., Zhao, P., Wu, C., Chen, K., Ren, W., Liu, L., Tang, Y., Ji, C., Sang, X., 2022. SIASAIL-I solar sail: From system design to on-orbit demonstration mission. Acta Astronaut. 192, 133–142. https://doi.org/10.1016/j.actaastro.2021.11.034.

Mu, J., Gong, S., Ma, P., Li, J., 2015. Dynamics and control of flexible spinning solar sails under reflectivity modulation. Adv. Space Res. 56, 1737–1751. https://doi.org/10.1016/j.asr.2015.07.028.

Quadrini, F., Bellisario, D., Iorio, L., Santo, L., 2019. Shape memory polymer composites by molding aeronautical prepregs with shape memory polymer interlayers. Mater. Res. Express 6 (11). https://doi.org/10.1088/2053-1591/ab50ad, art no 115711.

Quadrini, F., Iorio, L., Bellisario, D., Santo, L., 2021. Shape memory polymer composite unit with embedded heater. Smart Mater. Struct. 30 (7), 075009. https://doi.org/10.1088/1361-665X/ac00cb.

Quadrini, F., Iorio, L., Bellisario, D., Santo, L., 2022. Durability of shape memory polymer composite laminates under thermo-mechanical cycling. J. Compos. Sci. 6 (3), 91. https://doi.org/10.3390/jcs6030091.

Santo, L., Quadrini, F., Squeo, E.A., Dolce, F., Mascetti, G., Bertolotto, D., Villadei, W., Ganga, P.L., Zolesi, V., 2012. Behavior of shape memory epoxy foams in microgravity: Experimental results of STS-134 mission. Microgravity Sci. Technol. 24 (4), 287–296. https://doi.org/10.1007/s12217-012-9313-x.

Santo, L., Quadrini, F., Ganga, P.L., Zolesi, V., 2015. Mission BION-M1: Results of RIBES/FOAM2 experiment on shape memory polymer foams and composites. Aerosp. Sci. Technol. 40, 109–114. https://doi.org/10.1016/j.ast.2014.11.008.

Santo, L., Bellisario, D., Iorio, L., Quadrini, F., 2019. Shape memory composite structures for self-deployable solar sails. Astrodynamics 3 (3), 247–255. https://doi.org/10.1007/s42064-018-0044-7.

Santo, L., Quadrini, F., Bellisario, D., Iorio, L., Proietti, A., De Groh, K. K., 2024. Effect of the LEO space environment on the functional performances of shape memory polymer composites. Compos. Commun. 48101913. https://doi.org/10.1016/j.coco.2024.101913.

Seefeldt, P., 2017. A stowing and deployment strategy for large membrane space systems on the example of Gossamer-1. Adv. Space Res. 60 (6), 1345–1362. https://doi.org/10.1016/j.asr.2017.06.006.

Seefeldt, P., Spietz, P., Sproewitz, T., Thimo Grundmann, J., Hillebrandt, M., Hobbie, C., Ruffer, M., Straubel, M., To´th, N., Zander, M., 2017. Gossamer-1: Mission concept and technology for a controlled deployment of gossamer spacecraft. Adv. Space Res. 59 (1), 434–456. https://doi.org/10.1016/j.asr.2016.09.022S.

Seefeldt, P., Grundmann, J.T., Hillebrandt, M., Zander, M., 2021. Performance analysis and mission applications of a new solar sail concept based on crossed booms with tip-deployed membranes. Adv. Space Res. 67 (9), 2736–2745. https://doi.org/10.1016/j.asr.2020.10.001.

Sickinger, C., Herbeck, L., Breitbach, E., 2006. Structural engineering on deployable CFRP booms for a solar propelled sailcraft. Acta Astronaut. 58 (4), 185–196. https://doi.org/10.1016/j.actaastro.2005.09.011.

Spencer, D.A., Betts, B., Bellardo, J.M., Diaz, A., Plante, B., Mansell, J. R., 2021. The LightSail 2 solar sailing technology demonstration. Adv. Space Res. 67 (9), 2878–2889. https://doi.org/10.1016/j.asr.2020.06.029.

Spietz, P., Spröwitz, T., Seefeldt, P., et al., 2021. Paths not taken–The GOSSAMER roadmap's other options. Adv. Space Res. 67 (9), 2912–2956. https://doi.org/10.1016/j.asr.2021.01.044.

Tedde, G.M., Santo, L., Bellisario, D., Iorio, L., Quadrini, F., 2018. Frozen stresses in shape memory polymer composites. Materiale Plastice 55, 494–497. https://doi.org/10.37358/mp.18.4.5060.

Tsuda, Y., Mori, O., Funase, R., Sawada, H., Yamamoto, T., Saiki, T., Endo, T., Yonekura, K., Hoshino, H., Kawaguchi, J., 2013. Achievement of IKAROS-Japanese deep space solar sail demonstration mission. Acta Astronaut. 82 (2), 183–188. https://doi.org/10.1016/j.actaastro.2012.03.032.

Underwood, C., Viquerat, A., Schenk, M., et al., 2019. InflateSail de-orbit flight demonstration results and follow-on drag-sail applications. Acta Astronaut. 162, 344–358. https://doi.org/10.1016/j.actaastro.2019.05.054.

Wu, R., Roberts, P.C.E., Lyu, S., Soutis, C., Zheng, F., Diver, C., Gresil, M., Blaker, J.J., 2018. Rigidisation of deployable space polymer membranes by heat-activated self-folding. Smart Mater. Struct. 27 (10), 105037. https://doi.org/10.1088/1361-665X/aadc72.

Yang, H., Lu, F., Guo, H., Liu R., 2019b. Design of a New N-Shape Composite Ultra-Thin Deployable Boom in the Post-Buckling Range Using Response Surface Method and Optimization. IEEE Access, 7, art. no. 8794787, 129659-129665. doi: 10.1109/ACCESS.2019.2934744.

Yang, H., Liu, L., Guo, H., Lu, F., Liu, Y., 2019. Wrapping dynamic analysis and optimization of deployable composite triangular rollable and collapsible booms. Struct. Multidiscip. Optim. 59 (4), 1371–1383. https://doi.org/10.1007/s00158-018-2118-9.

Yang, H., Fan, S., Wang, Y., Shi, C., 2022. Novel four-cell lenticular honeycomb deployable boom with enhanced stiffness. Materials 15 (1), 306. https://doi.org/10.3390/ma15010306.

Zhang, X., Nie, R., Chen, Y., He, B., 2021. Deployable structures: structural design and static/dynamic analysis. J. Elast. 146 (2), 199–235. https://doi.org/10.1007/s10659-021-09860-6.

Zou, J., Li, D., Wang, J., Yu, Y., 2022. Experimental study of measuring the wrinkle of solar sails. Aerospace 9 (6), 289. https://doi.org/10.3390/aerospace9060289.